6-15-2022

Piperine derivatives enhance fusion and axonal transport of mitochondria by activating mitofusins

Lihong Zhang

Xiawei Dang

Antonietta Franco

Haiyan Zhao

Gerald W. Dorn II

chemistry

MDPI

Article

Piperine Derivatives Enhance Fusion and Axonal Transport of Mitochondria by Activating Mitofusins

Lihong Zhang [1,†], Xiawei Dang [2,†], Antonietta Franco [2], Haiyang Zhao [3] and Gerald W. Dorn II [1,*]

[1] Mitochondria in Motion, Inc., 4340 Duncan Ave, Suite 216, St. Louis, MO 63110, USA; lzhang25@wustl.edu
[2] Center for Pharmacogenomics, Department of Internal Medicine, Washington University School of Medicine, St. Louis, MO 63110, USA; x.dang@wustl.edu (X.D.); afranco@wustl.edu (A.F.)
[3] Department of Radiology, Washington University School of Medicine, St. Louis, MO 63110, USA; haiyangzhao2019@gmail.com
* Correspondence: gdorn@mimdrugs.com
† These authors contributed equally to this work.

Abstract: Piperine (1-piperoylpiperidine) is the major pungent component of black pepper (*Piper nigrum*) and exhibits a spectrum of pharmacological activities. The molecular bases for many of piperine's biological effects are incompletely defined. We noted that the chemical structure of piperine generally conforms to a pharmacophore model for small bioactive molecules that activate mitofusin (MFN)-mediated mitochondrial fusion. Piperine, but not its isomer chavicine, stimulated mitochondrial fusion in MFN-deficient cells with EC_{50} of ~8 nM. We synthesized piperine analogs having structural features predicted to optimize mitofusin activation and defined structure-activity relationships (SAR) in live-cell mitochondrial elongation assays. When optimal spacing was maintained between amide and aromatic groups the derivatives were potent mitofusin activators. Compared to the prototype phenylhexanamide mitofusin activator, **2**, novel molecules containing the piperidine structure of piperine exhibited markedly enhanced passive membrane permeability with no loss of fusogenic potency. Lead compounds **5** and **8** enhanced mitochondrial motility in cultured murine Charcot-Marie-Tooth disease type 2A (CMT2A) neurons, but only **8** improved mitochondrial transport in sciatic nerve axons of CMT2A mice. Piperine analogs represent a new chemical class of mitofusin activators with potential pharmaceutical advantages.

Keywords: piperine; mitochondrial fusion; mitochondrial transport; mitofusins; Charcot-Marie-Tooth disease

Citation: Zhang, L.; Dang, X.; Franco, A.; Zhao, H.; Dorn, G.W., II. Piperine Derivatives Enhance Fusion and Axonal Transport of Mitochondria by Activating Mitofusins. *Chemistry* **2022**, *4*, 655–668. https://doi.org/10.3390/chemistry4030047

Academic Editors: Barbara De Filippis and Gunter Peter Eckert

Received: 18 May 2022
Accepted: 15 June 2022
Published: 23 June 2022

1. Introduction

Piperine (1-(5-[1,3-benzodioxol-5-yl]-1-oxo-2,4-pentadienyl) piperidine) is responsible for the pungent taste of black pepper, other pepper species and ginger. Piperine is widely used in traditional medicine for anti-inflammatory and other beneficial properties in cancer, type 1 diabetes, inflammatory bowel disease, arthritis, asthma and liver disease (reviewed in [1–3]). Defining the molecular basis for piperine's biological activity has been of interest, both to understand its effects and to more specifically and successfully target defined effects in the context of modern medicine. Toward this end, over 15 different piperine molecular targets have been described [3,4], including mediators of altered drug bioavailability such as P-glycoprotein 1 (P-gp)/multidrug resistance protein 1 (MDR1) and intestinal CYP3A4 [5], modulators of neurotransmission such as γ-aminobutyric acid type A (GABAAR) receptors [6] and monoamine oxidase [7], and modulators of inflammation such as the human vanilloid receptor (TRPV1 channel) [8] and NF-kB [9]. Moreover, piperine has both direct and indirect effects on mitochondrial function [10,11]. However, piperine activity at the above targets typically requires micromolar concentrations and its use is limited by in vivo toxicity [12–14].

We wondered if previously described effects of piperine on mitochondrial function [10,11] might result from an interaction with an as-yet-unrecognized pharmacological target. Piperine has chemical similarities with some recently described novel small molecules that promote mitochondrial fusion by activating mitofusin (MFN) proteins [15,16]. Mitofusins initiate and mediate reparative mitochondrial fusion, and can regulate mitochondrial motility and quality control [17]. Thus, the untreatable genetic peripheral neuropathy Charcot-Marie-Tooth (CMT) disease type 2A, which is caused by mutations of MFN2, is characterized by abnormally short and hypomotile mitochondria [18,19]. Indeed, mitochondrial fragmentation and dysmotility have been described in many neurodegenerative conditions, but there are no clinical approaches to directly address these abnormalities [20]. For this reason, mitofusins have long been regarded as potential therapeutic targets whose activation could prove beneficial in CMT2A and other neurodegenerative conditions wherein impairments of mitochondrial fusion or motility are contributing factors. Here, we evaluated piperine effects on mitofusin-mediated mitochondrial elongation and polarization status and synthesized and characterized analogs that represent a new chemical class of mitofusin activators.

2. Materials and Methods

Detailed compound synthetic methods and chemical validation are in the Supplemental Materials; Supplemental Figures S1–S11.

Piperine (≥97% pure) was purchased from Sigma-Aldrich, St. Louis MO, USA (Cat# P49007). Chavicine (95% pure) was re-synthesized by Aurora Fine Chemicals.

Mitochondrial staining and imaging. Mitochondrial fusogenicity was measured using standard methods [15,16,21]. Briefly, mitochondrial elongation was assessed in Mfn2-deficient MEFs unless otherwise stated after adding compounds at concentrations ranging from 0.5 nM–10 μM in DMSO, overnight. Mfn2-deficient MEFs are commonly used to assay fusogenic activity because they have abnormally short mitochondria at baseline (due to absence of Mfn2) but respond to mitofusin activation with mitochondrial elongation mediated by normal endogenous Mfn1. Mitochondria were stained with MitoTracker Orange (excitation 549 nm, emission 590 nm; 200 nM; M7510; Invitrogen, Carlsbad, CA, USA). In some studies nuclei were co-stained with Hoechst (excitation 306 nm, emission 405 nm; 10 μg/mL; Invitrogen, Thermo Fisher Scientific Cat: # H3570). Mitochondrial aspect ratio (mitochondrial length/width) was measured from images acquired at room temperature on a Nikon Ti Confocal microscope using a 60 × 1.3 NA oil-immersion objective and analyzed using ImageJ. Compound fusogenicity, quantified as mitochondrial aspect ratio (mitochondrial length/width), was indexed to the maximal response elicited by the prototype mitofusin activator **2** [15,16]. Concentration-response curves were generated using a sigmoidal model in Prism 8 software. EC_{50} and E_{max} values and their variances were calculated from interpolated data of all replicate experiments in a series.

Mitochondrial polarization, which reflects integrity of the oxidative phosphorylation electron transport chain, was measured in wild-type, Mfn1-null, Mfn2-null, and Mfn1/Mfn2-double-null MEFs co-stained with Mito-tracker Green and tetra-methyl-rhodamine ester (TMRE, red). Fully polarized mitochondria stain both green and red (yellow/orange), whereas depolarized mitochondria fail to take up TMRE and appear green.

Mitochondrial motility in neuronal processes was measured using time-lapse confocal microscopy of dorsal root ganglion (DRG) neurons cultured from, or sciatic nerves explanted from, MFN2 T105M CMT2A mice as previously described [18]. For cultured DRGs, mitochondria were labelled by transduction with adenovirus-mitochondrial targeted RFP 48h prior to imaging; compounds were added in indicated concentrations ~18h prior to imaging. For ex vivo analyses of CMT2A mouse neurons, sciatic nerves including lumbar spine and extending to mid-tibia were excised and maintained briefly in tissue culture. Sciatic nerve mitochondria were labelled with TMRE (200 nM for 30 min at 37 °C) and visualized using time-lapse confocal microscopy (40 × water objective; 1 frame/5 s for 15 min). The % motile mitochondria was determined using kymographs generated

from line-scan confocal images of each frame of the time-lapse video, on which stationary mitochondria appear as vertical lines and motile mitochondria appear as diagonal lines.

In vitro pharmacokinetic assays. Plasma protein binding, liver microsome stability and passive artificial membrane permeability assay (PAMPA) studies were performed in duplicate by WuXi Apptec Co., Ltd. (Shanghai, China) using standard methods as described previously [15]. Briefly, compound binding to mouse and human plasma proteins was determined by equilibrium dialysis where % bound = (1 − [free compound in dialysate]/[total compound in retentate]) × 100. Compound (1 μM) stability in mouse and human liver microsomes (0.5 mg/mL) after 60 min incubation was determined by LC-MS/MS of extracted reactants. Passive artificial blood-brain barrier permeability (PAMPA-BBB) was measured 4 h after application of 150 μL of compounds (10 μM) to PVDF membranes coated with 1% porcine brain polar lipid extract with constant agitation at room temperature. Donor and acceptor samples were assayed using LC-MS/MS.

Synthetic Schemes. Chemical synthesis of novel compounds was accomplished as outlined in Synthetic Schemes 1–4. Detailed synthetic methods with NMR, HPLC, and LC-MS validation for each compound are in the Supplementary Materials.

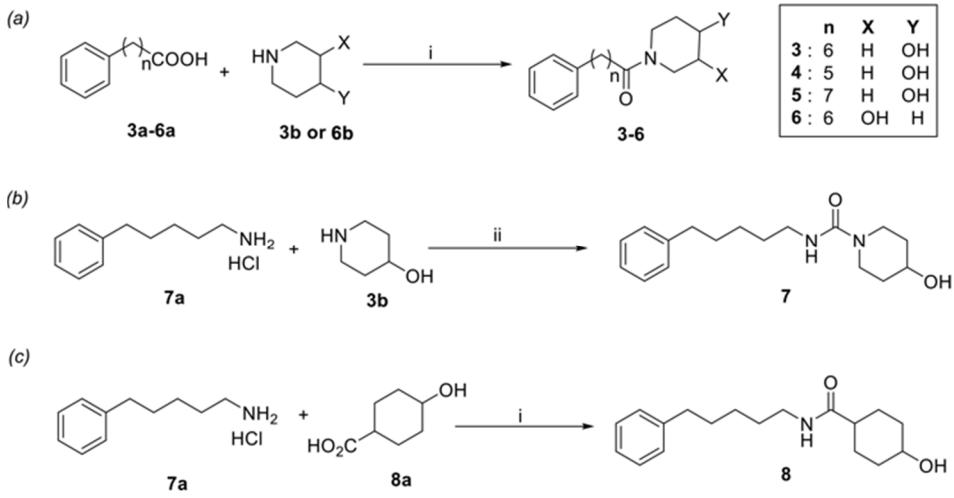

Scheme 1. Compounds 3–8: (**a**) **3–6**; (**b**) **7**; (**c**) **8**. *Reagents and conditions:* (i) HOBt (1.20 eq), EDCI (1.50 eq), DIEA (2.00 eq), DMF, 16 h, 30 °C. (ii) CDI (1.20 eq), TEA (3.00 eq), DMF, 16 h, 30 °C.

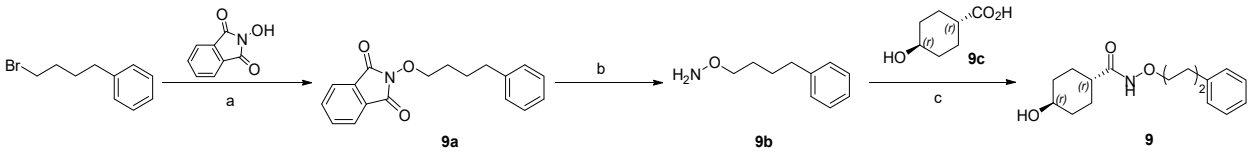

Scheme 2. Compound 9. Reagents and conditions: (a) K_2CO_3, DMF, 80 °C, 1 h. (b) NH_2-NH_2.H_2O, DCM, 25 °C, 2 h. (c) HATU, Et3N, THF, 25 °C, 2 h.

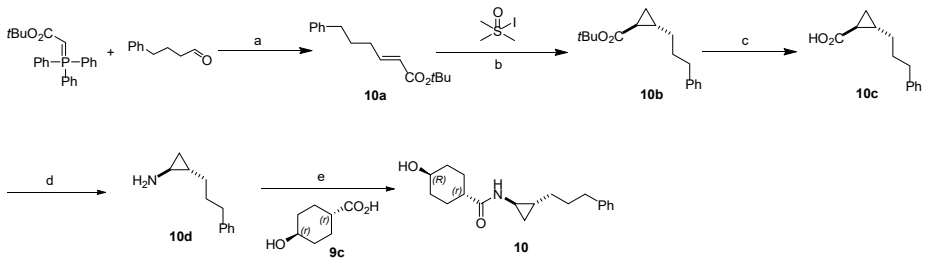

Scheme 3. Compound 10 *Reagents and conditions:* (a) THF, 12 h, 25 °C. (b) NaH, DMSO, 2 h, 25 °C. (c) TFA, DCM, 2 h, 25 °C. (d) DPPA, Et_3N, toluene, 105 °C, 2 h. (e) HATU, Et_3N, THF, 25 °C, 12 h.

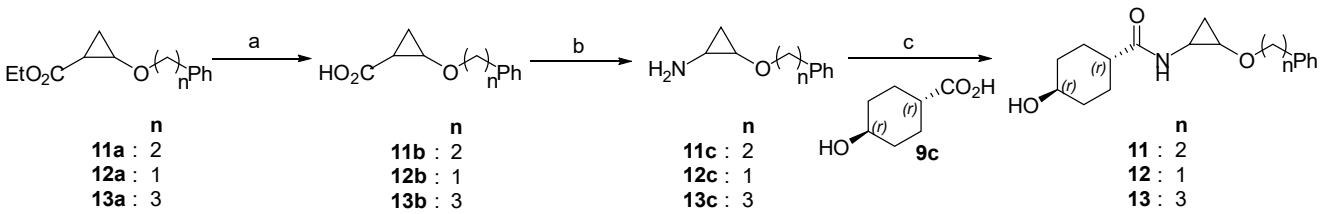

Scheme 4. Compounds 11–13. *Reagents and conditions*: (a) LiOH.H_2O, MeOH, THF/H_2O, 70 °C, 2 h. (b) DPPA, Et_3N, toluene, 105 °C, 2 h. (c) HATU, Et_3N, THF, 25 °C, 12 h.

Compounds **3**–**6** were obtained by the condensation reaction between the acids (**3a**–**6a**) and the amine (**3b** or **6b**) with moderate yield (Scheme 1a). Compounds **7** and **8** are prepared in one step using the commercially available 5-phenylpentylamine **7a** as the substrate (Scheme 1b,c).

Synthesis of compound **9**, a linker ether analog of compound **8**, used chiral **9c** as shown in Scheme 2. The hydroxylamine **9b** was prepared by two-step reaction with moderate yield. The chiral carboxylic acid **9c** is commercially available; the reaction between compound **9b** and the chiral carboxylic acid **9c** produced target compound **9**.

Compound **10** synthesis is shown in Scheme 3, coupling amine **10d** with chiral carboxylic acid **9c** using HATU in DMF. Amine **10d** was synthesized by converting 4-phenylbutanal starting compound to compound **10a** via the Wittig reaction. A cyclopropane group was introduced to create compound **10b**; after deprotecting the -tBu group, the ester **10b** was converted to the acid **10c**. The amine **10d** was obtained by the reaction between acid **10c** and DPPA.

Syntheses of compounds **11**–**13**, analogs of **10** in which a single methylene in the alkyl chain is replaced with oxygen, are shown in Scheme 4. Compounds **11a**–**13a** were prepared by converting to acids **11b**–**13b** under the conditions specified in Scheme 4. DPPA converted acids **11b**–**13b** to amines **11c**–**13c**. Compounds **11**–**13** were obtained by the reaction between amines **11c**–**13c** and **9c**.

Statistical methods. EC_{50} and E_{max} values are reported as means with 95% confidence limits or SEM. Intergroup comparisons used *t*-test, or ANOVA with Tukey's test for multiple groups. $p < 0.05$ was considered significant.

3. Results

Piperine is a mitofusin activator. We noted that the general chemical structure of piperine (**1**) is similar to that of a prototype phenylhexanamide small-molecule mitofusin activator (**2**; MiM111) [15] (Figure 1). Indeed, 3-dimensional stereochemical modeling showed similar molecular configurations corresponding to the previously reported mitofusin activator pharmacophore model [15]. In both compounds a 6-membered alkyl ring associated with a carboxamide is connected to a phenyl group or derivative by a 4–5 carbon linker.

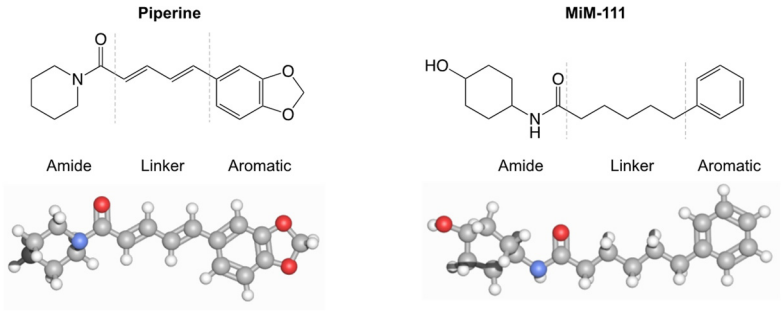

Figure 1. *Comparative structures of piperine and a prototype mitofusin activator.* (***top***) 2-dimensional structures without stereochemistry (ChemDraw). (***bottom***) 3-dimensional structures representing stereochemistry (ChemDoodle).

Published mitofusin activator structure-activity studies suggest that a cyclohexyl or heterocyclic carboxamide, a defined linker length, and an aromatic group are required for mitofusin activation. Within limits of the defining pharmacophore model, compounds with substitutions at the cyclohexyl, linker or phenyl groups retained functional potency while exhibiting different pharmacokinetic properties [15,16]. It is not known if piperine's piperidine amide structure can confer mitofusin stimulating activity.

Murine embryonic fibroblasts (MEFs) deficient in Mfn2 have characteristically short mitochondria as a consequence of chronically impaired mitochondrial fusion mediated by Mfn1 alone (Figure 2A). Mitofusin activators, such as **2**, promote mitochondrial fusion that elongates mitochondria in Mfn2-null MEFs (Figure 2A). Piperine (10^{-6} M) also stimulated mitochondrial elongation in Mfn2-null MEFs (Figure 2A), reflecting enhanced mitochondrial fusion [21]. As with previously described mitofusin activators [15,16], piperine's fusogenic activity appeared to slightly decrease at doses >1 μM, which may be attributable to loss of equipoise between mitofusin conformations, i.e., a propensity to stay in the unfolded conformation. Piperine's fusogenic potency (EC_{50}) and efficacy (E_{max}; maximum mitochondrial aspect ratio) were comparable to those of **2** studied in parallel (Figure 2B). Piperine's isomer chavicine (Supplemental Figure S12) lacked fusogenic activity (Figure 2), recapitulating stereoisomer-specific mitofusin activation reported for other small molecule mitofusin activators [15,16].

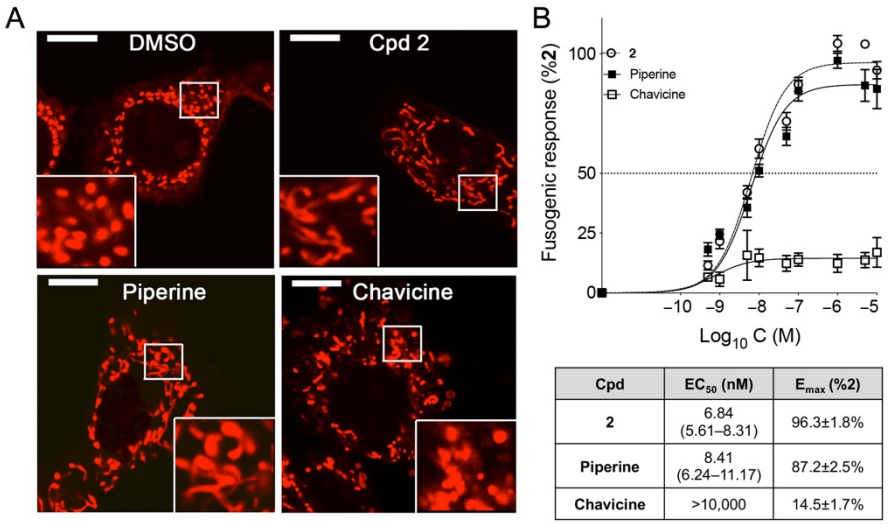

Cpd	EC_{50} (nM)	E_{max} (%2)
2	6.84 (5.61–8.31)	96.3±1.8%
Piperine	8.41 (6.24–11.17)	87.2±2.5%
Chavicine	>10,000	14.5±1.7%

Figure 2. Dose-dependent stimulatory effects of piperine on mitochondrial fusion in Mfn2-null MEFs. (**A**) Representative confocal images of MitoTracker orange-stained Mfn2-null MEFs after overnight treatment with DMSO vehicle (1:1000, left) or 1 μM Cpd **2**, piperine or chavicine. *Insets* are enlarged areas showing detailed mitochondrial morphology. Scale bars are 10 microns. (**B**) Concentration-response data for Cpd **2** (n = 8; open circles), piperine (n = 8; closed squares), and chavicine (n = 3; open squares) to increase mitochondrial length/width (aspect ratio) in Mfn2-null MEFs. Data are shown as means ± SEM. EC_{50} with 95% confidence intervals and E_{max} (% **2**) are below.

Mitochondrial elongation stimulated by piperine (100 nM, overnight) was similar in cells lacking either Mfn1 or Mfn2, but there was no fusogenic response when both mitofusins were absent (Figure 3, left). Thus, piperine's fusogenic effects require, and show equal activity for, Mfn1 or Mfn2. Like other mitofusin activators [15,16], piperine ameliorated the loss of mitochondrial polarization, which correlates with respiratory function in Mfn-deficient cells (Figure 3, right). Piperine caused a modest reduction in mitochondrial depolarization in cells lacking any mitofusin (Figure 3, right, Mfn 1/2 DKO), confirming prior reports that piperine can afford some degree of mitochondrial protection through mitofusin-independent processes [10,11]. Thus, piperine is a potent activator of Mfn1 and

Mfn2 at concentrations orders of magnitude less than its reported activities at GABA and vanilloid receptors, monoamine oxidase, and P-glycoprotein [5–8] (Table 1).

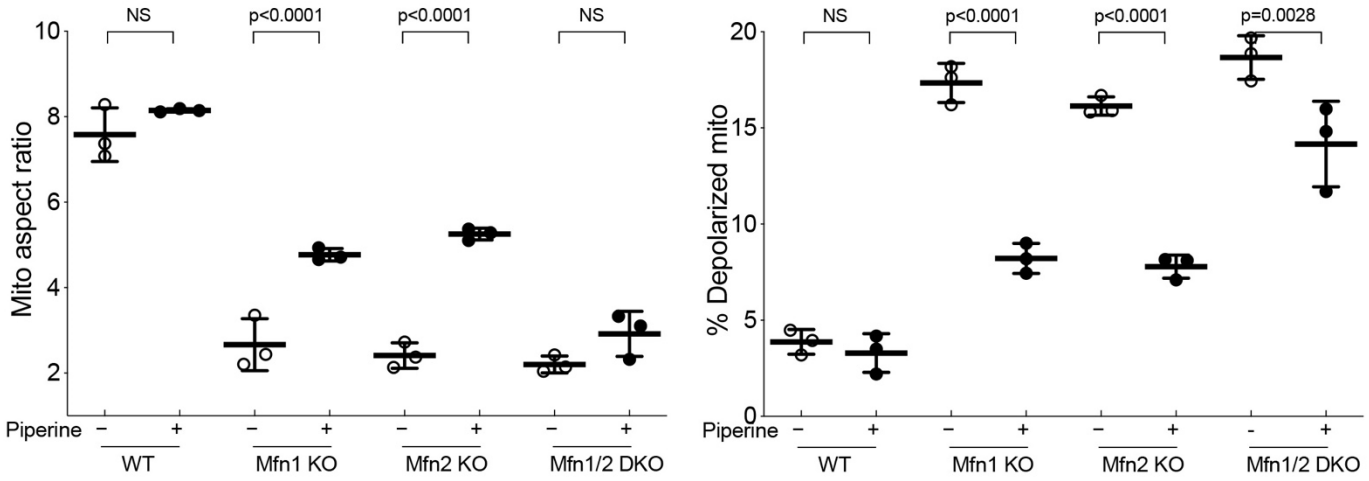

Figure 3. *Piperine screening in WT, Mfn1 KO (knockout), Mfn2 KO, and DKO (double knockout) MEFs.* Effects of piperine (100 nM) added to cells overnight were assessed on mitochondrial aspect ratio (**left**; MitoTracker Green staining) and depolarization (**right**; TMRE staining). Each point represents the average of 8–10 cells from one of three biological replicates. Means ± SEM are shown. *p* values used *t*-test.

Table 1. EC_{50}/IC_{50} values for piperine at reported targets.

Piperine Target	Action	EC_{50}/IC_{50} (nM)	Reference
Mitofusin	Activator	8	current paper
$GABA_AR$	Agonist	52,400	Schoffman *J Med Chem*
Vanilloid R (TRPV1)	Agonist	37,900	McNamara *Brit J Pharm*
P-gp/MDR1	Inhibitor	15,500; 74,100	Bhardwaj *JPET*
MAO-A	Inhibitor	20,900	Lee *Chem Pharm Bull*
MAO-B	Inhibitor	7000	"

Piperidine derivatives stimulate mitochondrial fusion. Aromatic groups of mitofusin activating compounds can be as simple as the phenyl group of **2** or as complex as the 5-cyclopropyl, 4-phenyl-1,2,4 triazole group of the original mitofusin activator chemical series [15,22]. Here, we retained the simple phenyl groupin combination with the hallmark piperidine moiety of piperine (**3**). In this piperidine series, linker flexibility was maximized with saturated carbon–carbon bonds, and linker size was decreased (**4**) or increased (**5**) by a single carbon to assess the consequences of different functional group spacing (Figure 4). In **6** the hydroxyl group on the piperidine ring was moved from the fourth to the third carbon.

Functional consequences of these chemical modifications were assessed on mitochondrial elongation in Mfn2-null MEFs, compared to prototype mitofusin activator **2** [**15**,**16**,**21**]. Like piperine, these novel piperidine analogs promoted mitochondrial fusion in Mfn2-deficient cells with potencies that changed according to linker length (Figure 5A,B; Cpds **3**–**5**). Moreover, repositioning the hydroxyl group from carbon 4 to carbon 3 of the piperidine ring markedly reduced fusogenic activity (Figure 5A,B; Cpd **6**); the 2-hydroxypiperidin derivative could not be synthesized.

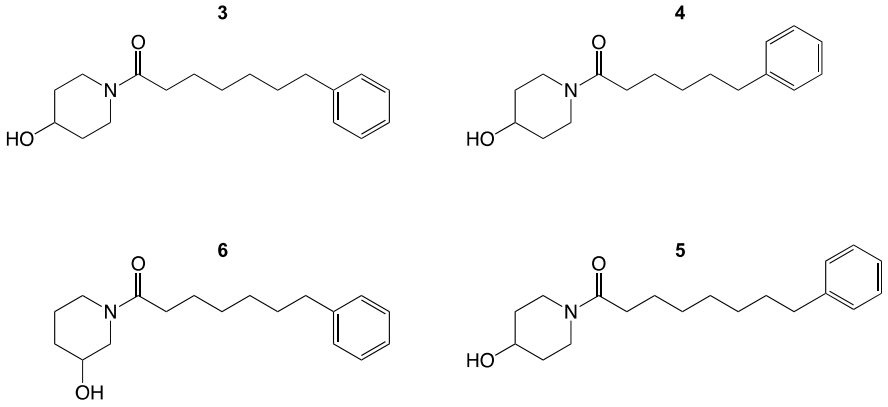

Figure 4. Piperidine analogs create a novel mitofusin activator scaffold.

Table 2. Functional and pharmacokinetic properties of piperidine variants.

Compound	2	3	4	5	6
MW	289.4	289.41	275.39	303.44	289.41
EC_{50} mito elongation mean (95% CI); nM	8.4 (6.1−11.4)	53.6 (22.4−ND)	>10,000	13.9 (8.5−21.8)	>10,000
Emax (% of 2) mean ± SEM	95.6 ± 2.9	54.0 ± 2.7	n/a	81.0 ± 3.7	37.0 ± 2.4
Plasma Protein Binding	% Bound	% Bound	% Bound	% Bound	% Bound
Human	91	95.1	83.7	98.6	96.6
Mouse	96.3	95.7	91.2	98.9	95.9
Liver Microsomes	T 1/2 (min)	T 1/2 (min)	T 1/2 (min)	T 1/2 (min)	T 1/2 (min)
Human	>145	103.3	>145	64.5	60.6
Mouse	92.4	52.5	82.4	26	22.5
PAMPA (Pe)	nm/s	nm/s	nm/s	nm/s	nm/s
	26.277	145.127	96.106	142.782	180.027

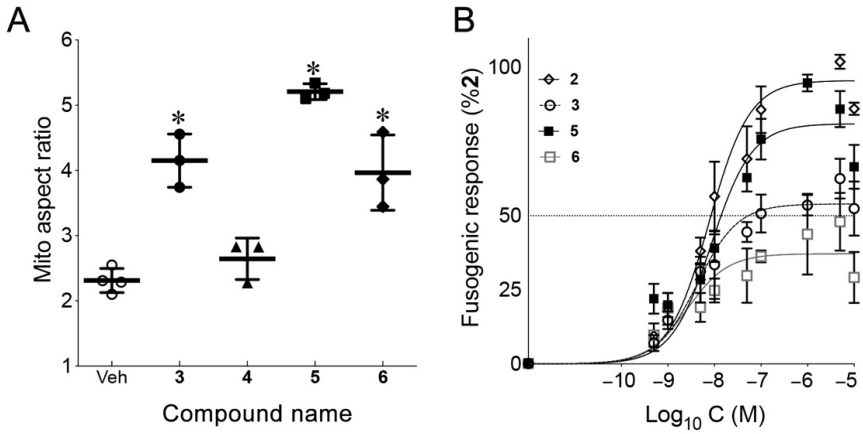

Figure 5. *Modulation of mitochondrial fusion by piperidine derivatives.* (**A**) Results of mitochondrial elongation screening assays performed in Mfn2-null MEFs using 1 μM of each piperidine derivative. (**B**) Concentration-dependent mitochondrial elongation of active compounds in Mfn2-null MEFs. EC_{50} with 95% CI and E_{max} values are in Table 2. * = $p < 0.05$ vsVeh.

Pharmacokinetic properties exhibited by piperidine analogs. The original triazolurea mitofusin activators and their derivatives exhibited a reciprocal relationship be-

tween hepatic microsome stability (that predicted plasma $t_{\frac{1}{2}}$) vs. passive membrane permeability (that predicted brain bioavailability) [15,22]. This compromised the utility of this chemical series for in vivo applications. Replacing the 5-cyclopropyl, 4-phenyl-1,2,4 triazole group with a simple phenyl ring helped stabilize the molecules, and additional stability was conferred by 4-hydroxy modification of the cyclohexyl group as in **2**. Compounds of this general phenylhexanamide structure exhibited passive membrane permeability, measured as PAMPA-BBB Pe, between 10 and 30 $\times$ 10^{-6} cm/s [15]. Compared to compound **2**, piperidine derivatives had comparable human and mouse plasma protein binding, but somewhat shorter half-lives in human and mouse hepatic microsome stability assays (Table 2). Strikingly, the piperidine analogs exhibited markedly increased PAMPA-BBB Pe, including of ~145 $\times$ 10^{-6} cm/sec for **3** and **5** that showed greatest fusogenic potency (Table 2).

Amide modifications. In the context of previously described urea- and carboxamide-based mitofusin activators [15,16,22], the current results with piperidine analogs suggested positional flexibility for the amide nitrogen in relation to the carbonyl group. To better understand the functional and pharmacokinetic consequences of amide nitrogen position we synthesized and characterized carbamide (**7**) and carboxamide (**8**) variants of **3** (Figure 6). Both compounds were markedly more potent and stable than **3**, while plasma protein binding did not meaningfully change. However, both amide variants had lower PAMPA-BBB Pe values compared to the piperidine (Table 3). Thus, increased potency and stability of these novel mitofusin activators were mitigated by reduced PAMPA permeability (and therefore the likelihood of decreased brain and oral bioavailability) when relative positions of the amide nitrogen and carbonyl groups were altered. Of the three compounds, the aggregate characteristics of **8** were closest to those of the prototype pharmaceutically acceptable mitofusin activator, **2** [15].

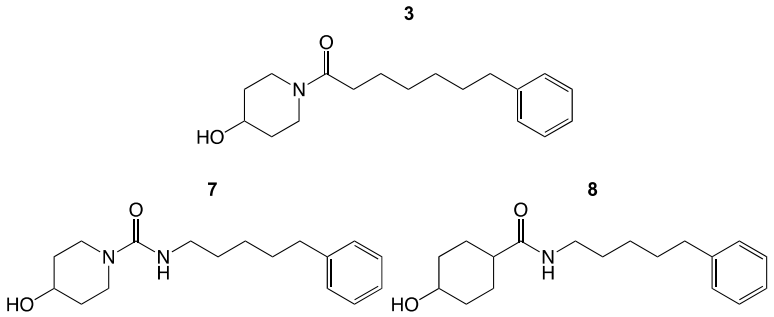

Figure 6. Amide variants of compound **3**.

Cyclopropyl linker modifications. Compounds **2** and **8** reflect chemical convergence of structure-function optimization efforts that began with entirely different parents, a triazolurea and piperine ([15]; current study). Indeed, **2** and **8** differ structurally only in the relative positions of the amide nitrogen and carboxyl (Figure 6); their fusogenic activity and pharmacokinetic profiles are also similar (Table 4). It was not surprising that chemically related compounds had alike characteristics, and this provided an opportunity to leverage prior SAR information derived from analogs of **2**, in which introduction of an ether or cycloalkyl group into the linker improved **2** passive permeability [15,16]. Accordingly, we synthesized and characterized variants of **8** having either a linker oxygen (**9**) or cyclopropyl group (**10**) adjacent to the amide nitrogen, corresponding to the most permeant, stable and potent analogs reported for **2** (Figure 7) [15,16].

Table 3. *Functional and pharmacokinetic properties of amide variants of **3**.* Values for **3** are duplicated from Table 2 for comparison.

Compound	**3**	**7**	**8**
MW	289.41	290.4	289.41
EC_{50} mito elongation mean (95% CI); nM	53.5 (22.4−ND)	4.7 (2.6−7.9)	13.5 (6.5−25.4)
Emax (% of 2)	54.0 ± 2.7	81.4 ± 4.0	69.4 ± 4.3
Plasma Protein Binding	% Bound	% Bound	% Bound
Human	95.1	91.7	89.3
Mouse	95.7	91.6	92.9
Liver Microsomes	T 1/2 (min)	T 1/2 (min)	T 1/2 (min)
Human	103.3	133.6	>145
Mouse	52.5	94.8	102.1
PAMPA (Pe)	nm/s	nm/s	nm/s
	145.127	14.585	30.249

Table 4. *Functional and pharmacokinetic properties of **8** linker variants.* **2** and **8** values are duplicated from Tables 2 and 3, respectively, for comparison.

Compound	**2**	**8**	**9**	**10**	**11**	**12**	**13**
MW	289.4	289.41	291.18	301.2	303.18	289.17	317.2
EC_{50} mito elongation mean (95% CI); nM	5.4 (4.1−7.1)	11.2 (6.3−19.2)	30.3 (18.9−47.2)	>10,000	10.6 (6.3−17.2)	10.8 (6.2−18.0)	27.0 (17.1−40.6)
Emax (% of 2)	94.3 ± 2.4	91.5 ± 5.1	65.4 ± 2.7	n/a	94.3 ± 4.7	75.6 ± 4.5	86.1 ± 3.3
Plasma Protein Binding	% Bound	% Bound	% Bound	% Bound	% Bound	% Bound	% Bound
Human	91	89.3	68.51	89.13	46.48	37.36	62.95
Mouse	96.3	92.9	unstable	95.34	72.14	63.93	77.92
Liver Microsomes	T 1/2 (min)	T 1/2 (min)	T 1/2 (min)	T 1/2 (min)	T 1/2 (min)	T 1/2 (min)	T 1/2 (min)
Human	>145	>145	10.3	>145	>145	>145	>145
Mouse	92.4	102.1	3.8	77.8	>145	>145	>145
PAMPA (Pe)	nm/s	nm/s	nm/s	nm/s	nm/s	nm/s	nm/s
	26.277	30.249	10.1	50.9	5.43	2.28	10.5

It is remarkable how much the consequences of linker modifications of **8** differed from the analogous modifications reported for **2**: The carbamate analog of **2** had an EC_{50} for mitochondrial elongation of 6 nM, a $t_{1/2}$ in human liver microsomes of 131 min., and PAMPA-BBB Pe of 210 × 10^{-6} cm/sec [15]. By comparison, **9**, which had a slightly higher EC_{50}, was unstable in the liver microsome assay and had much lower membrane permeability (Table 4). Moreover, the cyclopropyl linker analog of **2** had an EC_{50} of 5 nM, $t_{1/2}$ in human liver microsomes of >145 min., and a PAMPA-BBB Pe of 58 × 10^{-6} cm/sec [16], whereas the analogous **8** cyclopropyl linker analog, **10**, with comparable pharmacokinetics, had poor mitofusin-stimulating activity (Table 4, Figure 8). These results emphasize how chemical backbone/linker structure can be a major factor determining the pharmaceutical properties of mitofusin activators

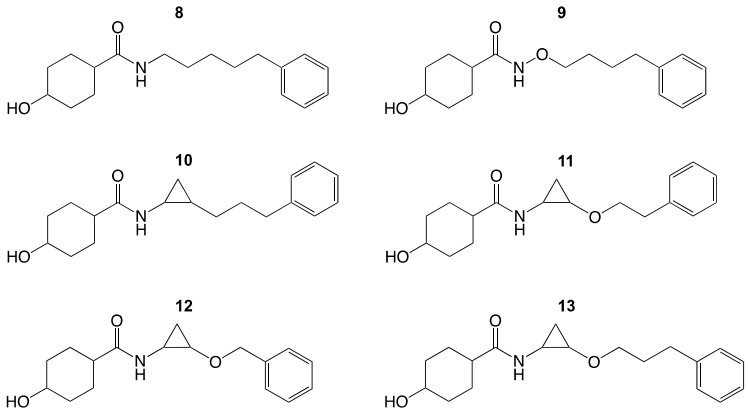

Figure 7. Linker variants of **8**.

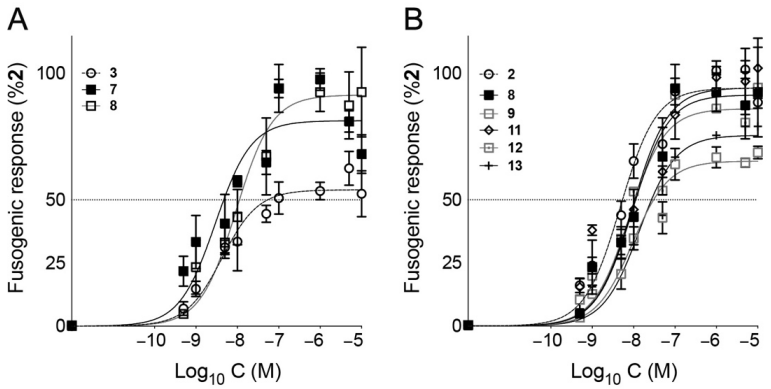

Figure 8. *Fusogenicity dose response curves for compounds reported in* Tables 3 and 4. (**A**) **3**, **7**, and **8** from Table 3. (**B**) **2**, **8**, **9**, **11**, **12**, and **13** from Table 4. **8** is duplicated for comparison.

There are no published data on how the combination of oxygen- and cycloalkyl-substituted linkers affects mitofusin activators. Accordingly, **11**, **12** and **13**, incorporating both modifications and differing only in linker size, were synthesized and characterized (Figure 7, Table 4). As previously observed, compound linker length determined fusogenic potency. In this series the longer linker, **13**, lost potency (Table 4). However, the major effects of incorporating an oxygen and cyclopropyl group into the linker were on pharmacokinetics. Compared to **8**, the ether linkages in **9** reduced plasma protein binding and PAMPA-BBB Pe. Also, the cyclopropyl group in **10** increased PAMPA-BBB vs. **8**. Combining ether/cycloalkyl linkers in **11**, **12** and **13** did not improve compound pharmaceutical characteristics.

Effects on mitochondrial motility in CMT2A neurons. As introduced above, Charcot-Marie-Tooth disease type 2A (CMT2A) is an untreatable progressive peripheral neuropathy caused by mutations of MFN2 [19,23,24]. Neurodegeneration in CMT2A is thought to result from a combination of impaired mitochondrial fusion and reduced mitochondrial motility in neuronal axons [20,25,26]; pharmacological mitofusin activation could be a potential disease-altering therapy for this condition. Here, because the piperidine **5** and the carboxamide **8** exhibited the most favorable combinations of in vitro functional and pharmacokinetic properties from their respective series, we examined their effects on mitochondrial motility in CMT2A.

Dorsal root ganglion (DRG) neurons were isolated from mice carrying a flox-stop transgene encoding the human CMT2A mutant MFN2 T105M; neuronal expression of MFN2 T105M in these mice recapitulates seminal features of clinical CMT2A, including a marked reduction in the proportion of motile mitochondria from the normal value of ~20% to ~5% [18]. As previously reported [18], **2** (100 nM for 48 h) reversed mitochondria dysmotility in MFN2 T105M DRGs (Figure 9A). Compounds **5** and **8** added at the

same concentration and for the same time period showed equivalent positive effects on mitochondrial motility (Figure 9A).

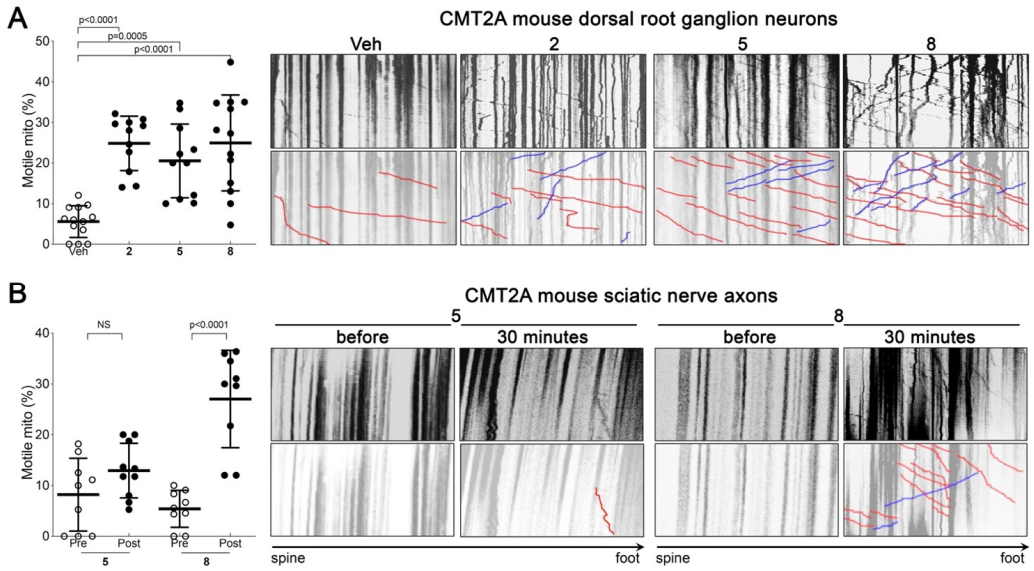

Figure 9. *Compound* **5** *and* **8** *effects on mitochondrial motility in CMT2A neurons.* (**A**) Experiments in cultured DRGs from MFN2 T105M Mice. (**left**) Group data. Each point is a different neuron, from two independent CMT2A mouse preparations; *p* values are from ANOVA. (**right**) representative kymographs of the different treatment groups. Top is raw data; bottom emphasizes motile mitochondria. (**B**) Experiments in explanted sciatic nerves from MFN2 T105M mice. (**left**) Group data before and 30 min after topical application of 1 μM indicated compound; *p* values are from *t*-test. (**right**) representative kymographs, as in (**A**).

Finally, we evaluated mitochondrial motility stimulation by **5** and **8** in axons of sciatic nerves explanted from MFN2 T105M flox-stop mice co-expressing motor-neuron-specific Cre recombinase. Topical application of a mitofusin activator to CMT2A sciatic nerves previously normalized mitochondrial motility within 30 min [22]. Here, **8** (1 μM) reproduced this effect, whereas **5** (1 μM) failed to evoke any significant increase in the proportion of motile mitochondria (Figure 9B). The ability of mitofusin activator **5** to stimulate mitochondrial motility in cultured murine CMT2A neurons, but not in ex vivo CMT2A mouse nerves, might be due to poor ability of the compound to access neurons through the intact nerve myelin sheath.

4. Discussion

Here, we report that piperine is a potent mitofusin activator at low nanomolar concentrations. Piperine stimulated mitochondrial fusion at concentrations multiple orders of magnitude lower than its reported effects on other known targets [27]. By implication, some of the reported biological activities of piperine, particularly those related to mitochondrial function or cellular metabolism [10,11], may be the consequence of mitofusin activation rather than other proposed mechanisms.

Mitochondrial fusion is a reparative process that maintains metabolic fitness by limiting the detrimental effects of mitochondrial DNA mutations or enzyme wear-and-tear that accumulate over time. In short, mitochondrial fusion helps prevent organelle senescence [17,28]. As mitochondrial dysfunction in some neurodegenerative and cardiac diseases might be causally linked to loss of mitochondrial fusion [20,29,30], there has been an effort to identify pharmacological means to promote reparative mitochondrial fusion and transport. Thus, leflunomide reportedly transcriptionally enhances mitofusin expression and 4-chloro-2-(1-(2-(2,4,6-trichlorophenyl)hydrazineylidene)ethyl)phenol is fusogenic [31,32], but micromolar EC_{50} values for both of these compounds limit their

clinical utility. Peptides and first-in-class small molecules that activate mitofusins through allosteric mechanisms were more potent, but had unfavorable pharmaceutical characteristics [15,21,22]. Indeed, the only pharmaceutically acceptable small-molecule mitofusin activators previously described are 6-phenylhexanamide derivatives [15,16].

The original triazolurea and second generation phenylhexanamide small-molecule mitofusin activators (and by inference piperine and its derivatives reported herein) reportedly increase mitofusin activity by disrupting peptide–peptide bonds that enforce a closed protein conformation unfavorable for mitochondrial fusion and transport [21,22,33,34]. This mechanism mimics the natural regulatory pathway in which the same MFN peptide–peptide interactions are modulated via phosphorylation/dephosphorylation reactions [35] and may explain lack of measurable toxicity for these compounds in cultured cells [15]. Likewise, phenylhexanamides, which can be given in vivo, have shown no adverse effects in mice [15,16,18]. Nevertheless, there are no published safety data in higher species and mitofusin activation has not been evaluated in human subjects. It is therefore important to identify new chemical classes of mitofusin activators, such as those described herein, as alternates to advance in case currently available compounds exhibit adverse effects. Moreover, expanding the universe of small-molecule mitofusin activators to include structurally diverse compounds exhibiting a spectrum of pharmacokinetic and pharmacodynamic properties will be central to properly evaluating the therapeutic potential of mitofusin activation beyond CMT2A. Thus, in addition to providing a plausible mechanism for mitochondrial and metabolic effects of piperine, the discovery that piperine and other piperidine compounds act as potent mitofusin activators is a foundational observation that can help establish a chemical framework for the possible development of novel mitofusin activators with new pharmaceutical properties.

Mitofusin activation represents the first potentially translatable means by which the novel and desirable therapeutic approach of enhancing mitochondrial dynamics can be evaluated in pre-clinical in vivo disease models. While CMT2A is the prototypical human disease caused by mitochondrial dynamic dysfunction, it is worth considering other applications for mitofusin activators. Mitochondrial fragmentation from impaired fusion or increased fission (or both) is a hallmark of such genetically and etiologically dissimilar neurological diseases as amyotrophic lateral sclerosis [36] and Huntington's disease [37], and mitochondrial damage caused in part by loss of mitofusin activity is thought to mediate chemotherapy-induced peripheral neuropathy [38,39]. Beyond the neurological system, mitofusin dysregulation is implicated in ischemic injury of the heart [40] and abnormalities of skin pigmentation [41,42].

The evolution of the novel compounds described herein leveraged chemical features of piperine, newly identified as a mitofusin activator, with lessons learned during the development of phenylhexanamide mitofusin activators [15]. It is notable that chemical modifications that improved the pharmaceutical properties of the latter (**2**) had strikingly different consequences in the reverse carboxamide (**8**) backbone described here. Indeed, ether, cyclopropyl and combined derivatives of **8** impaired PAMPA permeability except for **10**, which lacked meaningful fusogenic activity. By contrast, an analogous cyclopropyl derivative of **2** was previously identified as a potent, stable and longer-acting mitofusin activator suitable for pre-clinical evaluation [16]. Together with these published findings, the current results indicate that the amide position, while not itself critical to mitofusin activator functionality, can determine the consequences of secondary chemical modifications.

One other observation from the current study merits brief discussion. The dissociation of mitochondrial motility response for **5** in cultured neurons vs. intact nerves, while seemingly paradoxical, can be explained by impaired delivery of the compound across myelin sheaths and into neuronal axons. Myelin is produced by Schwann cells, which are not present in cultured DRG neuron preparations. Inability of a mitofusin activator to reach neurons would be a critical defect for treating CMT2A, but this characteristic might be useful for other clinical applications noted above. In a clinical context where the drug target is not the nervous system, avoiding potentially undesirable collateral effects of activating

mitofusins in neurons (such as mitochondrial hyper-motility that could possibly affect neuronal metabolism) would be consistent with the overall therapeutic goal.

Supplementary Materials: The following supporting information can be downloaded at: https://www.mdpi.com/article/10.3390/chemistry4030047/s1, Figures S1–S11: 1H NMR, HPLC and LC-MS chromatography of compounds; Figure S12: Piperine and chavicine structures.

Author Contributions: G.W.D.II conceived of the project, designed the compounds and experiments, interpreted data, and drafted the manuscript. L.Z. and X.D. performed experiments, analyzed data, and wrote the manuscript. A.F. performed experiments. H.Z. interpreted data and wrote the manuscript. All authors have read and agreed to the published version of the manuscript.

Funding: Supported by NINDS STTR grants R41NS113642 and R42NS115184 from the National Institute of Neurological Disorders and Stroke of the National Institutes of Health.

Data Availability Statement: All data reported are included in the manuscript and Supplementary Materials.

Acknowledgments: G.W.D.II holds the Philip and Sima K. Needleman Chair at the Washington University School of Medicine.

Conflicts of Interest: G.W.D. is the President and a Founder of Mitochondria in Motion, Inc., and is the inventor on multiple patents describing peptide and small molecule mitofusin activators and their potential uses in neurodegenerative diseases.

References

1. Darshan, S.; Doreswamy, R. Patented antiinflammatory plant drug development from traditional medicine. *Phytother. Res.* **2004**, *18*, 343–357. [CrossRef]
2. Derosa, G.; Maffioli, P.; Sahebkar, A. Piperine and Its Role in Chronic Diseases. *Adv. Exp. Med. Biol.* **2016**, *928*, 173–184. [CrossRef] [PubMed]
3. Stojanović-Radić, Z.; Pejčić, M.; Dimitrijević, M.; Aleksić, A.; Anil Kumar, N.V.; Salehi, B.; Cho, W.C.; Sharifi-Rad, J. Piperine-A Major Principle of Black Pepper: A review of its bioactivity and studies. *Appl. Sci.* **2019**, *9*, 4270. [CrossRef]
4. Meghwal, M.; Goswami, T.K. Piper nigrum and piperine: An update. *Phytother. Res.* **2013**, *27*, 1121–1130. [CrossRef] [PubMed]
5. Bhardwaj, R.K.; Glaeser, H.; Becquemont, L.; Klotz, U.; Gupta, S.K.; Fromm, M.F. Piperine, a major constituent of black pepper, inhibits human P-glycoprotein and CYP3A4. *J. Pharmacol. Exp. Ther.* **2002**, *302*, 645–650. [CrossRef] [PubMed]
6. Schöffmann, A.; Wimmer, L.; Goldmann, D.; Khom, S.; Hintersteiner, J.; Baburin, I.; Schwarz, T.; Hintersteininger, M.; Pakfeifer, P.; Oufir, M.; et al. Efficient modulation of γ-aminobutyric acid type A receptors by piperine derivatives. *J. Med. Chem.* **2014**, *57*, 5602–5619. [CrossRef]
7. Lee, S.A.; Hong, S.S.; Han, X.H.; Hwang, J.S.; Oh, G.J.; Lee, K.S.; Lee, M.K.; Hwang, B.Y.; Ro, J.S. Piperine from the fruits of Piper longum with inhibitory effect on monoamine oxidase and antidepressant-like activity. *Chem. Pharm. Bull.* **2005**, *53*, 832–835. [CrossRef]
8. McNamara, F.N.; Randall, A.; Gunthorpe, M.J. Effects of piperine, the pungent component of black pepper, at the human vanilloid receptor (TRPV1). *Br. J. Pharmacol.* **2005**, *144*, 781–790. [CrossRef]
9. Vaibhav, K.; Shrivastava, P.; Javed, H.; Khan, A.; Ahmed, M.E.; Tabassum, R.; Khan, M.M.; Khuwaja, G.; Islam, F.; Siddiqui, M.S.; et al. Piperine suppresses cerebral ischemia-reperfusion-induced inflammation through the repression of COX-2, NOS-2, and NF-κB in middle cerebral artery occlusion rat model. *Mol. Cell Biochem.* **2012**, *367*, 73–84. [CrossRef]
10. Selvendiran, K.; Thirunavukkarasu, C.; Singh, J.P.; Padmavathi, R.; Sakthisekaran, D. Chemopreventive effect of piperine on mitochondrial TCA cycle and phase-I and glutathione-metabolizing enzymes in benzo(a)pyrene induced lung carcinogenesis in Swiss albino mice. *Mol. Cell Biochem.* **2005**, *271*, 101–106. [CrossRef]
11. Kim, N.; Nam, M.; Kang, M.S.; Lee, J.O.; Lee, Y.W.; Hwang, G.S.; Kim, H.S. Piperine regulates UCP1 through the AMPK pathway by generating intracellular lactate production in muscle cells. *Sci. Rep.* **2017**, *7*, 41066. [CrossRef] [PubMed]
12. Piyachaturawat, P.; Glinsukon, T.; Toskulkao, C. Acute and subacute toxicity of piperine in mice, rats and hamsters. *Toxicol. Lett.* **1983**, *16*, 351–359. [CrossRef]
13. Allameh, A.; Saxena, M.; Biswas, G.; Raj, H.G.; Singh, J.; Srivastava, N. Piperine, a plant alkaloid of the piper species, enhances the bioavailability of aflatoxin B1 in rat tissues. *Cancer Lett.* **1992**, *61*, 195–199. [CrossRef]
14. Rao, P.J.; Kolla, S.D.; Elshaari, F.; Elshaari, F.; Awamy, H.E.; Elfrady, M.; Singh, R.; Belkhier, A.; Srikumar, S.; Said, A.R.; et al. Effect of piperine on liver function of CF-1 albino mice. *Infect. Disord. Drug Targets* **2015**, *15*, 131–134. [CrossRef]
15. Dang, X.; Zhang, L.; Franco, A.; Li, J.; Rocha, A.G.; Devanathan, S.; Dolle, R.E.; Bernstein, P.R.; Dorn, G.W., II. Discovery of 6-Phenylhexanamide Derivatives as Potent Stereoselective Mitofusin Activators for the Treatment of Mitochondrial Diseases. *J. Med. Chem.* **2020**, *63*, 7033–7051. [CrossRef]

16. Dang, X.; Williams, S.B.; Devanathan, S.; Franco, A.; Fu, L.; Bernstein, P.R.; Walters, D.; Dorn, G.W., II. Pharmacophore-Based Design of Phenyl-[hydroxycyclohexyl] Cycloalkyl-Carboxamide Mitofusin Activators with Improved Neuronal Activity. *J. Med. Chem.* **2021**, *64*, 12506–12524. [CrossRef]
17. Dorn, G.W., II. Mitofusin 2 Dysfunction and Disease in Mice and Men. *Front. Physiol.* **2020**, *11*, 782. [CrossRef]
18. Franco, A.; Dang, X.; Walton, E.K.; Ho, J.N.; Zablocka, B.; Ly, C.; Miller, T.M.; Baloh, R.H.; Shy, M.E.; Yoo, A.S.; et al. Burst mitofusin activation reverses neuromuscular dysfunction in murine CMT2A. *eLife* **2020**, *9*, e61119. [CrossRef]
19. Züchner, S.; Mersiyanova, I.V.; Muglia, M.; Bissar-Tadmouri, N.; Rochelle, J.; Dadali, E.L.; Zappia, M.; Nelis, E.; Patitucci, A.; Senderek, J.; et al. Mutations in the mitochondrial GTPase mitofusin 2 cause Charcot-Marie-Tooth neuropathy type 2A. *Nat. Genet.* **2004**, *36*, 449–451. [CrossRef]
20. Knott, A.B.; Perkins, G.; Schwarzenbacher, R.; Bossy-Wetzel, E. Mitochondrial fragmentation in neurodegeneration. *Nat. Rev. Neurosci.* **2008**, *9*, 505–518. [CrossRef]
21. Franco, A.; Kitsis, R.N.; Fleischer, J.A.; Gavathiotis, E.; Kornfeld, O.S.; Gong, G.; Biris, N.; Benz, A.; Qvit, N.; Donnelly, S.K.; et al. Correcting mitochondrial fusion by manipulating mitofusin conformations. *Nature* **2016**, *540*, 74–79. [CrossRef] [PubMed]
22. Rocha, A.G.; Franco, A.; Krezel, A.M.; Rumsey, J.M.; Alberti, J.M.; Knight, W.C.; Biris, N.; Zacharioudakis, E.; Janetka, J.W.; Baloh, R.H.; et al. MFN2 agonists reverse mitochondrial defects in preclinical models of Charcot-Marie-Tooth disease type 2A. *Science* **2018**, *360*, 336–341. [CrossRef] [PubMed]
23. Feely, S.M.; Laura, M.; Siskind, C.E.; Sottile, S.; Davis, M.; Gibbons, V.S.; Reilly, M.M.; Shy, M.E. MFN2 mutations cause severe phenotypes in most patients with CMT2A. *Neurology* **2011**, *76*, 1690–1696. [CrossRef] [PubMed]
24. Pipis, M.; Feely, S.M.E.; Polke, J.M.; Skorupinska, M.; Perez, L.; Shy, R.R.; Laura, M.; Morrow, J.M.; Moroni, I.; Pisciotta, C.; et al. Natural history of Charcot-Marie-Tooth disease type 2A: A large international multicentre study. *Brain* **2020**, *143*, 3589–3602. [CrossRef]
25. Chen, H.; Chan, D.C. Mitochondrial dynamics fusion, fission, movement, and mitophagy in neurodegenerative diseases. *Hum. Mol. Genet.* **2009**, *18*, R169–R176. [CrossRef]
26. Misko, A.L.; Sasaki, Y.; Tuck, E.; Milbrandt, J.; Baloh, R.H. Mitofusin2 mutations disrupt axonal mitochondrial positioning and promote axon degeneration. *J. Neurosci.* **2012**, *32*, 4145–4155. [CrossRef]
27. Singh, I.P.; Choudhary, A. Piperine and Derivatives: Trends in Structure-Activity Relationships. *Curr. Top. Med. Chem.* **2015**, *15*, 1722–1734. [CrossRef]
28. Song, M.; Franco, A.; Fleischer, J.A.; Zhang, L.; Dorn, G.W., II. Abrogating Mitochondrial Dynamics in Mouse Hearts Accelerates Mitochondrial Senescence. *Cell Metab.* **2017**, *26*, 872–883. [CrossRef]
29. Dorn, G.W., II; Vega, R.B.; Kelly, D.P. Mitochondrial biogenesis and dynamics in the developing and diseased heart. *Genes Dev.* **2015**, *29*, 1981–1991. [CrossRef]
30. Dang, X.; Walton, E.K.; Zablocka, B.; Baloh, R.H.; Shy, M.E.; Dorn, G.W., II. Mitochondrial Phenotypes in Genetically Diverse Neurodegenerative Diseases and Their Response to Mitofusin Activation. *Cells* **2022**, *11*, 1053. [CrossRef]
31. Wang, D.; Wang, J.; Bonamy, G.M.; Meeusen, S.; Brusch, R.G.; Turk, C.; Yang, P.; Schultz, P.G. A small molecule promotes mitochondrial fusion in mammalian cells. *Angew. Chem. Int. Ed. Engl.* **2012**, *51*, 9302–9305. [CrossRef] [PubMed]
32. Miret-Casals, L.; Sebastián, D.; Brea, J.; Rico-Leo, E.M.; Palacín, M.; Fernández-Salguero, P.M.; Loza, M.I.; Albericio, F.; Zorzano, A. Identification of New Activators of Mitochondrial Fusion Reveals a Link between Mitochondrial Morphology and Pyrimidine Metabolism. *Cell Chem. Biol.* **2018**, *25*, 268–278.e264. [CrossRef] [PubMed]
33. Dorn, G.W., II. Evolving Concepts of Mitochondrial Dynamics. *Annu. Rev. Physiol.* **2019**, *81*, 1–17. [CrossRef] [PubMed]
34. Dorn, G.W., II. Mitofusins as mitochondrial anchors and tethers. *J. Mol. Cell Cardiol.* **2020**, *142*, 146–153. [CrossRef]
35. Li, J.; Dang, X.; Franco, A.; Dorn, G.W., II. Reciprocal Regulation of Mitofusin 2-Mediated Mitophagy and Mitochondrial Fusion by Different PINK1 Phosphorylation Events. *Front. Cell Dev. Biol.* **2022**, *10*, 868465. [CrossRef]
36. Wang, L.; Gao, J.; Liu, J.; Siedlak, S.L.; Torres, S.; Fujioka, H.; Huntley, M.L.; Jiang, Y.; Ji, H.; Yan, T.; et al. Mitofusin 2 Regulates Axonal Transport of Calpastatin to Prevent Neuromuscular Synaptic Elimination in Skeletal Muscles. *Cell Metab.* **2018**, *28*, 400–414.e408. [CrossRef]
37. Kim, J.; Moody, J.P.; Edgerly, C.K.; Bordiuk, O.L.; Cormier, K.; Smith, K.; Beal, M.F.; Ferrante, R.J. Mitochondrial loss, dysfunction and altered dynamics in Huntington's disease. *Hum. Mol. Genet.* **2010**, *19*, 3919–3935. [CrossRef]
38. Bobylev, I.; Joshi, A.R.; Barham, M.; Neiss, W.F.; Lehmann, H.C. Depletion of Mitofusin-2 Causes Mitochondrial Damage in Cisplatin-Induced Neuropathy. *Mol. Neurobiol.* **2018**, *55*, 1227–1235. [CrossRef]
39. Yamashita, Y.; Irie, K.; Kochi, A.; Kimura, N.; Hayashi, T.; Matsuo, K.; Myose, T.; Sano, K.; Nakano, T.; Takase, Y.; et al. Involvement of Charcot-Marie-Tooth disease gene mitofusin 2 expression in paclitaxel-induced mechanical allodynia in rats. *Neurosci. Lett.* **2017**, *653*, 337–340. [CrossRef]
40. Hall, A.R.; Burke, N.; Dongworth, R.K.; Kalkhoran, S.B.; Dyson, A.; Vicencio, J.M.; Dorn, G.W., II; Yellon, D.M.; Hausenloy, D.J. Hearts deficient in both Mfn1 and Mfn2 are protected against acute myocardial infarction. *Cell Death Dis.* **2016**, *7*, e2238. [CrossRef]
41. Daniele, T.; Hurbain, I.; Vago, R.; Casari, G.; Raposo, G.; Tacchetti, C.; Schiaffino, M.V. Mitochondria and melanosomes establish physical contacts modulated by Mfn2 and involved in organelle biogenesis. *Curr. Biol.* **2014**, *24*, 393–403. [CrossRef] [PubMed]
42. Tanwar, J.; Saurav, S.; Basu, R.; Singh, J.B.; Priya, A.; Dutta, M.; Santhanam, U.; Joshi, M.; Madison, S.; Singh, A.; et al. Mitofusin-2 Negatively Regulates Melanogenesis by Modulating Mitochondrial ROS Generation. *Cells* **2022**, *11*, 701. [CrossRef] [PubMed]